JGSP **33** (2014) 27–45

JOURNAL OF
Geometry and Symmetry in Physics
ISSN 1312-5192

A NATURAL PARAMETERIZATION OF THE ROULETTES OF THE CONICS GENERATING THE DELAUNAY SURFACES

ENRIQUE BENDITO, MARK J. BOWICK AND AGUSTÍN MEDINA

Communicated by John Oprea

Abstract. We derive parametrizations of the Delaunay constant mean curvature surfaces of revolution that follow directly from parametrizations of the conics that generate these surfaces via the corresponding roulette. This uniform treatment exploits the natural geometry of the conic (parabolic, elliptic or hyperbolic) and leads to simple expressions for the mean and Gaussian curvatures of the surfaces as well as the construction of new surfaces.

1. Preliminaries

The surfaces of revolution with constant mean curvature (CMC) were introduced and completely characterized by C. Delaunay more than a century ago [4]. Delaunay's formulation of the problem leads to a non–linear ordinary differential equation involving the radius of curvature of the plane curve that generates the surface, which can be also characterized variationally as the surface of revolution having a minimal lateral area with a fixed volume (see [6]). Delaunay showed that the above differential equation arises geometrically by rolling a conic along a straight line without slippage. The curve described by a focus of the conic, the *roulette of the conic*, is then the meridian of a surface of revolution with constant mean curvature, where the straight line is the axis of revolution. These CMC surfaces of revolution are called *Delaunay surfaces*. Apart from the elementary cases of spheres and cylinders, there are three classes of Delaunay surfaces, the *catenoids*, the *unduloids* and the *nodoids*, corresponding to the choice of conic as a parabola, an ellipse or a hyperbola, respectively.

Traditionally the roulettes have been characterized using polar coordinates centered at the focus of the conic [3, 6–8, 10–13]. The methods employed in these papers are based on solving certain ordinary differential equations that, in one way or another, depend on the variational characterization of the CMC surfaces. Although reference [3] does suggest the possibility of using the cartesian coordinates of the roulettes with the tangent to the conic as the abscissa, this idea is never developed.

doi: 10.7546/jgsp-33-2014-27-45

Here we obtain parametrizations of the roulettes, and therefore of the corresponding Delaunay surfaces, directly from the parametrizations of the conics. This leads directly to concise expressions for all the key differential geometric characteristics of Delaunay surfaces. In our approach the unduloid is described with trigonometric functions, whereas the catenoid and the nodoid are described with hyperbolic functions. This yields simple expressions for the Gaussian curvature, total curvature and mean curvature as well as the length of roulettes. The mean curvature of an unduloid, in particular, is given by the inverse of the distance between the vertices of the corresponding ellipse, whereas the mean curvature of a nodoid is given by minus the inverse of the distance between the vertices of the corresponding hyperbola. The parametrizations presented here also give rise to a straightforward construction of nodoids, both when viewed as simple parts (generated by a focus) or when they are composed of several individual parts or a periodic repetition of simple parts.

For the sake of completeness, we finish this section by presenting some well-known results about regular surfaces of revolution, as well as a very simple proof of the Gauss-Bonett theorem for this class of surfaces.

Let $f,g:[t_1,t_2]\longrightarrow\mathbb{R}$ be smooth functions with $f>0$, and S the surface of revolution parametrized by $\boldsymbol{x}:[t_1,t_2]\times[v_1,v_2]\longrightarrow\mathbb{R}^3$

$$\boldsymbol{x}(t,v)=\Big(f(t)\cos(v),f(t)\sin(v),g(t)\Big)$$

The coefficients of the first and second fundamental forms of S are given by

$$\begin{aligned}
&E=\langle\boldsymbol{x}_t,\boldsymbol{x}_t\rangle=(f')^2+(g')^2, && F=\langle\boldsymbol{x}_t,\boldsymbol{x}_v\rangle=0, \quad G=\langle\boldsymbol{x}_v,\boldsymbol{x}_v\rangle=f^2\\
&L=\langle\boldsymbol{x}_{tt},\boldsymbol{n}\rangle=\frac{f'g''-f''g'}{\Big((f')^2+(g')^2\Big)^{1/2}}, && M=\langle\boldsymbol{x}_{tv},\boldsymbol{n}\rangle=0\\
&N=\langle\boldsymbol{x}_{vv},\boldsymbol{n}\rangle=\frac{fg'}{\Big((f')^2+(g')^2\Big)^{1/2}}
\end{aligned}$$

where

$$\boldsymbol{n}=\frac{\boldsymbol{x}_t\times\boldsymbol{x}_v}{|\boldsymbol{x}_t\times\boldsymbol{x}_v|}=\frac{1}{\Big((f')^2+(g')^2\Big)^{1/2}}\Big(-g'\cos(v),-g'\sin(v),f'\Big)$$

is the unit normal to S. The Gaussian curvature is given by

$$K=\frac{LN}{EG}=\frac{g'\big(f'g''-f''g'\big)}{f\Big((f')^2+(g')^2\Big)^2}$$

whereas the mean curvature, H, is given by

$$2H = k_1 + k_2 = \frac{L}{E} + \frac{N}{G} = \frac{f'g'' - f''g'}{\Big((f')^2 + (g')^2\Big)^{3/2}} + \frac{g'}{f\Big((f')^2 + (g')^2\Big)^{1/2}}$$

where k_1 and k_2 are the two principal curvatures.

Now consider a curve α in S parametrized by the arc length s. For any point $p = \alpha(s)$ we choose a vector $\boldsymbol{u}(s)$ in the tangent space at p such that $\{\alpha'(s), \boldsymbol{u}(s)\}$ is a positively oriented orthonormal basis of the tangent space at p, i.e., $\alpha'(s) \times \boldsymbol{u}(s) = \boldsymbol{n}(\alpha(s))$. The geodesic curvature $k_g(s)$ of α at s is then given by

$$k_g(s) = \langle \alpha''(s), \boldsymbol{u}(s) \rangle.$$

If the curve is chosen to be a meridian of S, $\alpha(t) = \boldsymbol{x}(t, v_0)$, then $k_g = 0$, whereas if it is a parallel, $\beta(v) = \boldsymbol{x}(t_0, v)$, then its geodesic curvature is given by

$$k_g(t_0) = \frac{f'(t_0)}{f(t_0)\Big((f'(t_0))^2 + (g'(t_0))^2\Big)^{1/2}}.$$

Lemma 1. *If C_1 and C_2 are the boundary parallels of S with the orientation induced by S then*

$$\int_S K \mathrm{d}\sigma + \int_{C_1} k_g(t_1)\mathrm{d}\ell + \int_{C_2} k_g(t_2)\mathrm{d}\ell = 0.$$

Proof: Observe first that $k_g(t)|\boldsymbol{x}_v| = \dfrac{f'(t)}{\Big((f'(t))^2 + (g'(t))^2\Big)^{1/2}}$ and hence

$$\Big(k_g|\boldsymbol{x}_v|\Big)' = \frac{g'\Big(f''g' - f'g''\Big)}{\Big((f')^2 + (g')^2\Big)^{3/2}} = -K|\boldsymbol{x}_t|\,|\boldsymbol{x}_v|.$$

On the other hand

$$\begin{aligned}\int_S K\mathrm{d}\sigma &= \int_{v_1}^{v_2}\int_{t_1}^{t_2} K|\boldsymbol{x}_t|\,|\boldsymbol{x}_v|\mathrm{d}t\mathrm{d}v = -\int_{v_1}^{v_2}\int_{t_1}^{t_2}\Big(k_g|\boldsymbol{x}_v|\Big)'\mathrm{d}t\mathrm{d}v \\ &= \int_{v_1}^{v_2} k_g(t_1)|\boldsymbol{x}_v(t_1,v)|\mathrm{d}v - \int_{v_1}^{v_2} k_g(t_2)|\boldsymbol{x}_v(t_2,v)|\mathrm{d}v \\ &= -\int_{C_1} k_g(t_1)\mathrm{d}\ell - \int_{C_2} k_g(t_2)\mathrm{d}\ell.\end{aligned}$$

In the case of coordinate intervals of surfaces of revolution, using this lemma, we may conclude the Gauss-Bonnet Theorem ([5], p 274), because if $v_2 - v_1 = 2\pi$, then the sum of external angles is zero, so S is homeomorphic to an annulus with null Euler characteristic. Otherwise, it is a simple region whose Euler characteristic equals 1 and the sum of the external angles at the four boundary vertices, formed by the tangents to the boundary curves oriented with the orientation induced by S, equals 2π.

2. The Roulettes of the Conics

When a curve rolls, without slipping, on a fixed curve, each point, associated with the rolling curve, traces another curve known as a *roulette*. In Fig. 1 (left), we show the trace generated by the point $F = (F_1, F_2)$, associated with a given curve C, when it rolls on a straight line. The abscissa F_1 of the roulette coincides with Q_1, i.e., the length of the arc of the curve from P_o to P, minus the value $P_1 - Q_1$ (where P_1, Q_1 are the abscisae of the points P, Q respectively). We can interchange the roles of the conic and its tangent by considering a fixed conic and a moving tangent. The locus of the points Q thus obtained is called the *pedal curve* of C with respect to F.

Consider the plane curve C given by $f(x, y) = 0$, the point $F = (A, B)$, the tangent line of coordinates X, Y at the point $P = (x, y)$ of the curve is

$$(r_T): \qquad \frac{X}{f_y} + \frac{Y}{f_x} - \frac{x}{f_y} - \frac{y}{f_x} = 0$$

and the perpendicular line to (r_T) passing through F

$$(r_T^{\perp}): \qquad \frac{X}{f_x} - \frac{Y}{f_y} - \frac{A}{f_x} + \frac{B}{f_y} = 0.$$

Then

$$d(Q, F) = d(r_T, F) = \frac{|(A - x)f_x + (B - y)f_y|}{\sqrt{f_x^2 + f_y^2}}$$

$$d(Q, P) = d(r_T^{\perp}, P) = \frac{|(B - y)f_x + (x - A)f_y|}{\sqrt{f_x^2 + f_y^2}}.$$

Here we are interested in the roulettes generated by the conic foci when they roll over a tangent line. The cartesian and parametric description of the *parabola*, the *ellipse* and the *hyperbola* are given respectively by

$$\begin{aligned} x - \frac{y^2}{4b} &= 0, & \alpha(t) &= \big(b\sinh^2(t), 2b\sinh(t)\big) \\ \frac{x^2}{a^2} + \frac{y^2}{b^2} &= 1, & \beta(t) &= \Big(a\cos(t), b\sin(t)\Big) \\ \frac{x^2}{a^2} - \frac{y^2}{b^2} &= 1, & \gamma(t) &= \Big(\pm\, a\cosh(t), b\sinh(t)\Big) \end{aligned}$$

where $a, b > 0$ and $t \in [t_1, t_2] \subset \mathbb{R}$.

In Fig. 1 (right), we show a parabola, with the perpendicular from F onto the tangent of the parabola at P. This situation is equivalent to the general case and we apply the same criteria to give a parameterization of this roulette. The focus with this parameterization is $F = (b, 0)$.

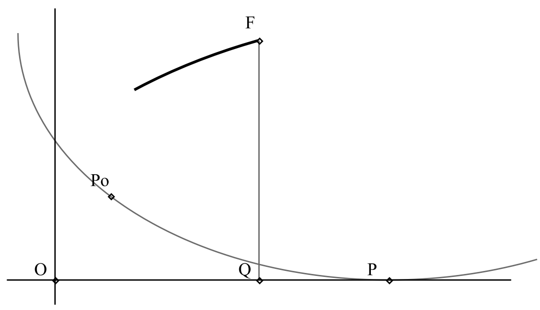

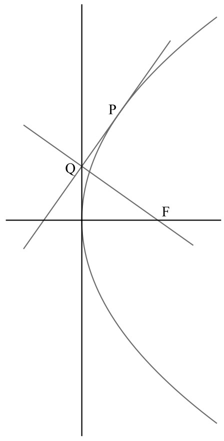

Figure 1. Roulette (left) and Parabola (right).

The arc length of the piece of the parabola from $t_0 = 0$ is $s = \displaystyle\int_{t_0}^{t} |\alpha'(u)|\mathrm{d}u = b(t + \sinh(t)\cosh(t))$, and the length of the segment $\overline{PQ}$ is $d(Q, P) = \dfrac{|y(b + x)|}{\sqrt{y^2 + 4b^2}} = |b\sinh(t)\cosh(t)|$. Note that, if $t < t_0$, the value of s is negative, and the relative positions of P and Q in (r_T) are changed. Then the value of the abscissa, that is the oriented tangent line (r_T), is the signed length s minus the signed length to go from P to Q, that is

$$g_c(t) = s - b\sinh(t)\cosh(t) = bt. \tag{1}$$

Computing the ordinate $f_c(t)$ (that is, the length of the segment $\overline{FQ}$), i.e.,

$$f_c(t) = d(Q, F) = \frac{1}{2}\sqrt{y^2 + 4b^2} = b\cosh t \tag{2}$$

we conclude that the roulette associated with the focus of the parabola is the *catenary*

$$A(t) = (g_c(t), f_c(t)) = (bt, b\cosh(t)).$$

Note also that

$$|A'(t)| = b\cosh(t)$$

and the arc length is given by

$$\ell_c(t) = \int_{t_0}^{t} |A'(z)|\,\mathrm{d}z = b\sinh(z)\Big|_{t_0}^{t}.$$

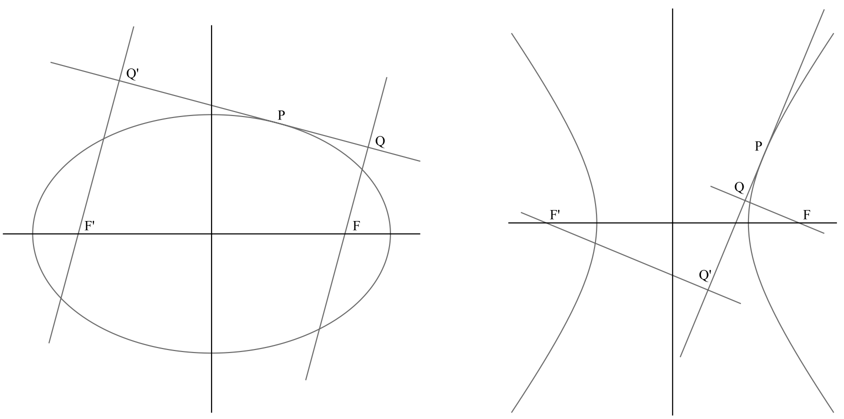

Figure 2. Ellipse (left) and Hyperbola (right).

For the ellipse, Fig. 2 (left), take $b < a$ and $c = \sqrt{a^2 - b^2}$. The focus with this parameterization is $F = (c, 0)$. The arc length from t_0 is

$$s = \int_{t_0}^{t} |\beta'(z)|\mathrm{d}z = \int_{t_0}^{t} \sqrt{a^2 - c^2\cos^2(z)}\,\mathrm{d}z.$$

In this case two curves are generated. The first one corresponds to choosing the focus F closest to the tangent. By computing the length of the segment $\overline{PQ}$,

$d(Q,P) = \dfrac{|cy(a^2-cx)|}{\sqrt{a^4y^2+b^4x^2}} = \dfrac{|c\sin(t)(a-c\cos(t))|}{\sqrt{a^2-c^2\cos^2(t)}}$, the abscissa of the roulette is the length s minus the signed length to go from P to Q, that is

$$g_u(t) = \int_{t_0}^{t} \sqrt{a^2-c^2\cos^2(z)}\mathrm{d}z - \frac{c\sin(t)\,(a-c\cos(t))}{\sqrt{a^2-c^2\cos^2(t)}}. \tag{3}$$

In addition, the ordinate is given by the length of the segment $\overline{FQ}$, $d(Q,F) = \dfrac{b^2(a^2-cx)}{\sqrt{a^4y^2+b^4x^2}}$, namely

$$f_u(t) = \frac{b\,(a-c\cos(t))}{\sqrt{a^2-c^2\cos^2(t)}} \tag{4}$$

and $B(t) = (g_u(t), f_u(t))$ is therefore the parametrization of the roulette generated by the focus of the ellipse. One finds

$$|B'(t)| = \frac{ab}{a+c\cos(t)}$$

and the arc length is given by

$$\ell_u(t) = \int_{t_0}^{t} |B'(z)|\mathrm{d}z = 2a\arctan\left(\sqrt{\frac{a-c}{a+c}}\tan\left(\frac{z}{2}\right)\right)\Big|_{t_0}^{t}.$$

In the same way, if we chooose the other focus $F' = (-c, 0)$, it follows after computing the length of $\overline{PQ'}$ that the abscissa is

$$\tilde{g}_u(t) = \int_{t_0}^{t} \sqrt{a^2-c^2\cos^2(z)}\mathrm{d}z - \frac{c\sin(t)\,(a+c\cos(t))}{\sqrt{a^2-c^2\cos^2(t)}} \tag{5}$$

and the ordinate is the length of the segment $\overline{F'Q'}$, namely

$$\tilde{f}_u(t) = \frac{b\,(a+c\cos(t))}{\sqrt{a^2-c^2\cos^2(t)}} \tag{6}$$

and $\tilde{B}(t) = (\tilde{g}_u(t), \tilde{f}_u(t))$ is therefore the parametrization of the roulette generated by the focus F'. One now finds

$$|\tilde{B}'(t)| = \frac{ab}{a-c\cos(t)}$$

and an arc length

$$\tilde{\ell}_u(t) = \int_{t_0}^{t} |\tilde{B}'(z)|\mathrm{d}z = 2a\arctan\left(\sqrt{\frac{a+c}{a-c}}\tan\left(\frac{z}{2}\right)\right)\Big|_{t_0}^{t}.$$

Observe in particular that $\arctan\left(\sqrt{\frac{a+c}{a-c}}\right) + \arctan\left(\sqrt{\frac{a-c}{a+c}}\right) = \pi/2$ and then the sum of the length of the two curves for $t \in (-\pi/2, \pi/2)$ is $2\pi a$.

The roulette of the focus of an ellipse is called an *undulary*. It is clear that we do not need to consider both foci for an ellipse. Specifically, if we consider the ellipse described by taking $t \in [-\pi, \pi]$, the curve generated by the focus F is the same as the curve that results from joining the two curves generated by both foci F and F' with $t \in [-\pi/2, \pi/2]$ only. We consider both foci to make manifest the constructive parallelism between these roulettes and the roulettes of the hyperbola.

Consider now the case of the hyperbola, as shown Fig. 2 (right). Taking $c = \sqrt{a^2 + b^2}$. The focus with this parameterization is $F = (c, 0)$. The arc length from t_0 to t is

$$s = \int_{t_0}^{t} |\gamma'(z)| \mathrm{d}z = \int_{t_0}^{t} \sqrt{c^2 \cosh^2(z) - a^2}\, \mathrm{d}z.$$

For the first roulette we consider the focus F closest to the tangent. By computing the length of the segment $\overline{PQ}$ in a similar manner to the preceding cases, it then follows that the abscissa is

$$g_n(t) = \int_{t_0}^{t} \sqrt{c^2 \cosh^2(z) - a^2}\, \mathrm{d}z - \frac{c \sinh(t)\,(c \cosh(t) - a)}{\sqrt{c^2 \cosh^2(t) - a^2}} \tag{7}$$

whereas its ordinate is given by the length of $\overline{FQ}$, namely

$$f_n(t) = \frac{b\,(c \cosh(t) - a)}{\sqrt{c^2 \cosh^2(t) - a^2}} \tag{8}$$

and therefore $C(t) = (g_n(t), f_n(t))$ is the parametrization of the roulette generated by the focus F. One finds

$$|C'(t)| = \frac{ab}{c \cosh(t) + a}$$

with arc length given by

$$\ell(t) = \int_{t_0}^{t} |C'(z)| \mathrm{d}z = 2a \arctan\left(\sqrt{\frac{c-a}{c+a}} \tanh\left(\frac{z}{2}\right)\right)\Bigg]_{t_0}^{t}.$$

In particular, the length of C with $t \in (-\infty, \infty)$ is $4a \arctan\left(\sqrt{\frac{c-a}{c+a}}\right)$.

Taking the focus $F' = (-c, 0)$ instead one finds, after computing the length of $\overline{PQ'}$, that the abscissa is

$$\tilde{g}_n(t) = \int_{t_0}^{t} \sqrt{c^2 \cosh^2(z) - a^2}\, \mathrm{d}z - \frac{c \sinh(t)\,(c \cosh(t) + a)}{\sqrt{c^2 \cosh^2(t) - a^2}} \tag{9}$$

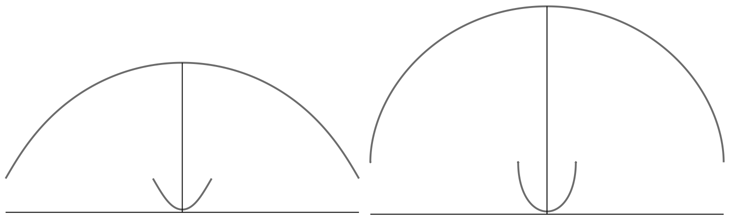

Figure 3. Roulettes B and $\tilde{B}$ (left) and roulettes C and $\tilde{C}$ (right).

and the ordinate is the length of the segment $\overline{F'Q'}$, namely

$$\tilde{f}_n(t) = \frac{b\,(c\cosh(t) + a)}{\sqrt{c^2\cosh^2(t) - a^2}} \tag{10}$$

which gives us the parameterization $\tilde{C}(t) = (\tilde{g}_n(t), \tilde{f}_n(t))$ of the roulette generated by the focus F'. Now

$$|\tilde{C}'(t)| = \frac{ab}{c\cosh(t) - a}$$

and the arc length is given by

$$\tilde{\ell}(t) = \int_{t_0}^{t} |\tilde{C}'(z)|\mathrm{d}z = 2a\arctan\left(\sqrt{\frac{c+a}{c-a}}\tanh\left(\frac{z}{2}\right)\right)\Bigg]_{t_0}^{t}.$$

The sum of the length of the two branches of the curves for $t \in (-\infty, \infty)$ is again $2\pi a$. The roulette of the focus of a hyperbola is called a *nodary*.

In Fig. 3 we display the roulettes generated by the foci of the ellipse (left) and the hyperbola (right). B and C are the curves with increasing slope, while $\tilde{B}$ and $\tilde{C}$ are the curves with decreasing slope.

In Fig. 4 we display the pedal curves of the ellipse (left) and of the hyperbola (right). Both are circles of diameter equal to the distance between the vertices of the conic. It is known that when a curve rolls on a straight line the arc of the roulette is equal to the corresponding arc of the pedal. Here we can see this directly. If we consider, for instance, the curve C and denote $x = \arctan\left(\sqrt{\frac{c-a}{c+a}}\right)$, then

$$\sin(2x) = \frac{b}{c}, \qquad \cos(2x) = \frac{a}{c}$$

and so

$$4a\arctan\left(\sqrt{\frac{c-a}{c+a}}\right) = 2a\arctan\left(\frac{b}{a}\right).$$

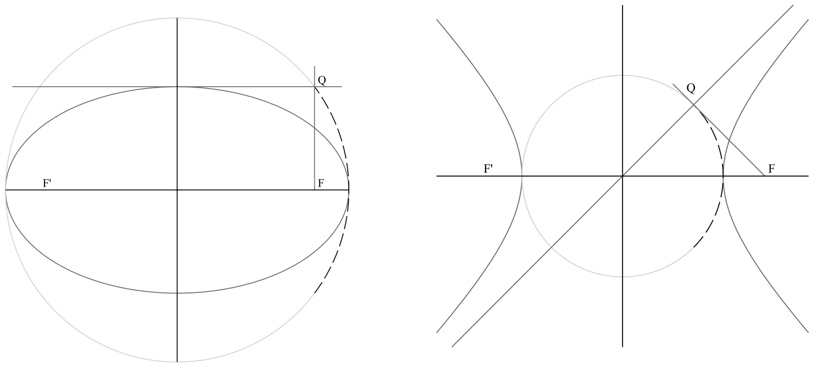

Figure 4. Pedal curves of the ellipse and the hyperbola. Left: arc of the circle (dash), whose length coincides with the length of the curve B and arc of the circle, whose length coincides with the length of the curve $\tilde{B}$. Right: arc of the circle (dash), whose length coincides with the length of the curve C and arc of the circle whose length coincides with the length of the curve $\tilde{C}$.

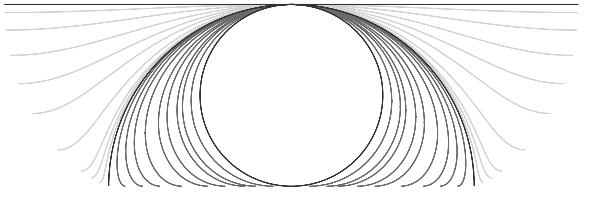

Figure 5. Family of roulettes $B \cup \tilde{B}$ and $C \cup \tilde{C}$ of length $2\pi a$.

That is, the length of the curve C coincides with the length of the associated pedal curve – see Fig. 4 (right).

In Fig. 5 we display a family of roulettes with length $2\pi a$. Each of these roulettes was generated by a conic with major axis a. The straight segment corresponds to a curve of type B in the limiting case $b = a$. This is followed by a set of elliptical roulettes from $b = a$ until the next limiting case $b = 0$, corresponding to a semicircumference of radius $2a$. The remaining roulettes correspond to curves of type C, ranging from the limiting case $b = 0$, again the same semicircumference, until $b = \infty$, which is the circle of radius a shown in the figure.

In Fig. 6 (left) we show the same family of roulettes shown in Fig. 5, but to the height, with respect to the abscissa axis, at which it has been generated by the focus of the corresponding conic. Observe that the limiting circumference of radius a

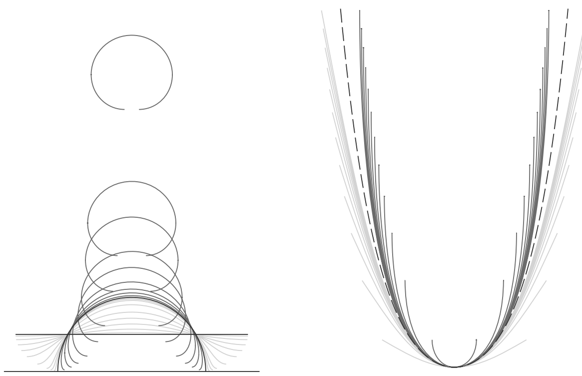

Figure 6. Left: Location of the roulettes in Fig. 5 with respect to the abscissa axis. Right: a family of roulettes of type B and C separated by a catenary (dash).

would have the center at height $b = \infty$. In Fig. 6 (right) we display the asymptotic role of the catenary separating two families of curves B and C. In this case the corresponding conics do not have the parameter a constant, and both families tend to the catenary as the parameter a grows.

3. The Delaunay Surfaces

In this section we study Delaunay surfaces and derive analytical expressions for their most important differential geometric properties. The Delaunay surfaces are surfaces of revolution and therefore the key to their properties lie in their meridians, which here are the roulettes of the foci of the conics discussed in the previous section. The Delaunay surfaces are thus the surfaces of revolution generated by the curves $A(t)$, $B(t)$, $\tilde{B}(t)$, $C(t)$ and $\tilde{C}(t)$. We next describe the parametrization, the coefficients of the first and second fundamental forms of each one of these surfaces and their curvatures. The entire differential structure has a remarkably transparent dependence on the parameters that characterize each conic.

CATENOID: $\boldsymbol{x}(t,v) = \Big(f_c(t)\cos(v), f_c(t)\sin(v), g_c(t)\Big)$, where f_c and g_c are given in equations (2) and (1) respectively, see Fig. 7. We have

$$\boldsymbol{x}_t = (b\sinh(t)\cos(v), b\sinh(t)\sin(v), b)$$

$$\boldsymbol{x}_v = (-b\cosh(t)\sin(v), b\cosh(t)\cos(v), 0)\,.$$

The unit normal vector at (t, v) is given by

$$\boldsymbol{n}_c(t,v) = \left(-\frac{\cos(v)}{\cosh(t)}, -\frac{\sin(v)}{\cosh(t)}, \tanh(t)\right).$$

The non–vanishing coeficients of the first and the second fundamental form, and the principal curvatures, the mean curvature and the Gaussian curvature are

$$\begin{array}{llll} E = b^2\cosh^2(t), & G = b^2\cosh^2(t), & L = -b, & N = b \\ k_1 = \dfrac{-1}{b\cosh^2(t)}, & k_2 = \dfrac{1}{b\cosh^2(t)}, & H = 0, & K = \dfrac{-1}{b^2\cosh^4(t)}. \end{array}$$

The geodesic curvature of a parallel is

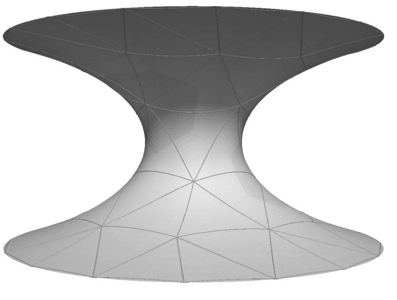

Figure 7. The catenoid.

$$k_g = \frac{\sinh(t)}{b\cosh^2(t)}$$

and the total curvature of the catenoid is

$$\int_{\boldsymbol{x}} K \mathrm{d}\sigma = -(v_2 - v_1)\tanh(t)\Big|_{t_1}^{t_2}.$$

UNDULOID: $\boldsymbol{y}(t,v) = \Big(f_u(t)\cos(v), f_u(t)\sin(v), g_u(t)\Big)$, where f_u and g_u are given in equations (4) and (3) respectively, see Fig. 8 (left). Introducing

$$h_u(t) = \frac{ab}{\sqrt{a^2 - c^2\cos^2(t)}\,(a + c\cos(t))}$$

it follows that

$$\begin{aligned}\boldsymbol{y}_t &= (c\sin(t)h_u(t)\cos(v), c\sin(t)h_u(t)\sin(v), bh_u(t))\\ \boldsymbol{y}_v &= (-f_u(t)\sin(v), f_u(t)\cos(v), 0)\,.\end{aligned}$$

The machinary of the differential geometry [5] in this case produces the unit normal vector

$$\boldsymbol{n}_u(t,v) = \left(\frac{-b\cos(v)}{\sqrt{a^2 - c^2\cos^2(t)}}, \frac{-b\sin(v)}{\sqrt{a^2 - c^2\cos^2(t)}}, \frac{c\sin(t)}{\sqrt{a^2 - c^2\cos^2(t)}}\right)$$

and

$$\begin{aligned}
E &= \frac{a^2b^2}{(a + c\cos(t))^2}, & G &= \frac{b^2\,(a - c\cos(t))}{(a + c\cos(t))}\\
L &= \frac{-ab^2c\cos(t)}{(a^2 - c^2\cos^2(t))\,(a + c\cos(t))}, & N &= \frac{b^2}{a + c\cos(t)}\\
k_1 &= \frac{-c\cos(t)}{a(a - c\cos(t))}, & k_2 &= \frac{1}{a - c\cos(t)}\\
H &= \frac{1}{2a}, & K &= \frac{-c\cos(t)}{a\,(a - c\cos(t))^2}.
\end{aligned}$$

Correspondingly, the geodesic curvature of a parallel is

$$k_g = \frac{-c\sin(t)}{b\big(a - c\cos(t)\big)}$$

and the total curvature is

$$\int_{\boldsymbol{y}} K\mathrm{d}\sigma = -c(v_2 - v_1)\frac{\sin(t)}{\sqrt{a^2 - c^2\cos^2(t)}}\Bigg|_{t_1}^{t_2}.$$

Clearly one could do the same calculation for the surface generated by $\tilde{B}$ (see Fig 8 (right)), but it is enough consider the proper domain of the parameter t to belong to one or another part of the unduloid. In fact these surfaces are periodic with period 2π with respect to the parameter t.

We must, however, consider both parts C and $\tilde{C}$ in the construction of the nodoids, because each roulette has its domain in $\Re$.

NODOID1: $\boldsymbol{z}_1(t,v) = \Big(f_n(t)\cos(v), f_n(t)\sin(v), g_n(t)\Big)$, where f_n and g_n are given in equations (8) and (7) respectively, see Fig. 9 (left). We consider

$$h_1(t) = \frac{ab}{\sqrt{c^2\cosh^2(t) - a^2}\,(c\cosh(t) + a)}$$

Figure 8. Unduloids generated by the revolution of B (left), and $\tilde{B}$ (right).

from which it follows that

$$\begin{aligned}(\boldsymbol{z}_1)_t &= \Big(c\sinh(t)h_1(t)\cos(v), c\sinh(t)h_1(t)\sin(v), bh_1(t)\Big)\\ (\boldsymbol{z}_1)_v &= \Big(-f_n(t)\sin(v), f_n(t)\cos(v), 0\Big).\end{aligned}$$

The unit normal vector at (t,v) is given by

$$\boldsymbol{n}_1(t,v) = \left(\frac{-b\cos(v)}{\sqrt{c^2\cosh^2(t)-a^2}}, \frac{-b\sin(v)}{\sqrt{c^2\cosh^2(t)-a^2}}, \frac{c\sinh(t)}{\sqrt{c^2\cosh^2(t)-a^2}}\right).$$

Respectively, the fundamental quantities in this case are

$$\begin{aligned}
E &= \frac{a^2b^2}{(c\cosh(t)+a)^2}, & G &= \frac{b^2\,(c\cosh(t)-a)}{c\cosh(t)+a}\\
L &= \frac{-ab^2c\cosh(t)}{\big(c^2\cosh^2(t)-a^2\big)\,(c\cosh(t)+a)}, & N &= \frac{b^2}{c\cosh(t)+a}\\
k_1 &= \frac{-c\cosh(t)}{a(c\cosh(t)-a)}, & k_2 &= \frac{1}{c\cosh(t)-a}\\
H &= \frac{-1}{2a}, & K &= \frac{-c\cosh(t)}{a\,(c\cosh(t)-a)^2}.
\end{aligned}$$

The geodesic curvature of a parallel is

$$k_g = \frac{c\sinh(t)}{b\big(c\cosh(t)-a\big)}$$

and the total curvature is

$$\int_{\boldsymbol{z}_1} K\mathrm{d}\sigma = -c(v_2-v_1)\left.\frac{\sinh(t)}{\sqrt{c^2\cosh^2(t)-a^2}}\right|_{t_1}^{t_2}.$$

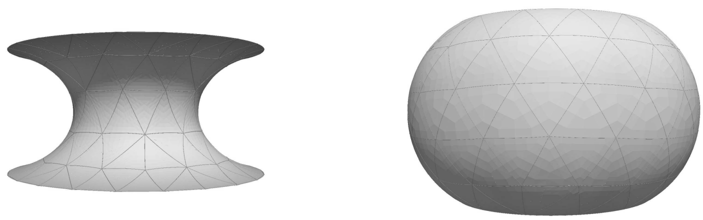

Figure 9. Nodoids generated by the revolution of C (left) and $\tilde{C}$ (right).

NODOID2: $\boldsymbol{z}_2(t,v) = \Big(\tilde{f}_n(t)\cos(v), \tilde{f}_n(t)\sin(v), \tilde{g}_n(t)\Big)$, where $\tilde{f}_n$ and $\tilde{g}_n$ are given in equations (10) and (9) respectively, see Fig. 9 (right). Let us introduce

$$h_2(t) = \frac{-ab}{\sqrt{c^2\cosh^2(t) - a^2}\,(c\cosh(t) - a)}$$

from which it follows that

$$\begin{aligned}(\boldsymbol{z}_2)_t &= \Big(c\sinh(t)h_2(t)\cos(v)c\sinh(t)h_2(t)\sin(v), bh_2(t)\Big)\\ (\boldsymbol{z}_2)_v &= \Big(-\tilde{f}_n(t)\sin(v), \tilde{f}_n(t)\cos(v), 0\Big).\end{aligned}$$

This allows to find easily the unit normal vector

$$\boldsymbol{n}_2(t,v) = \left(\frac{b\cos(v)}{\sqrt{c^2\cosh^2(t) - a^2}}, \frac{b\sin(v)}{\sqrt{c^2\cosh^2(t) - a^2}}, -\frac{c\sinh(t)}{\sqrt{c^2\cosh^2(t) - a^2}}\right)$$

and

$$\begin{aligned}E &= \frac{a^2b^2}{(c\cosh(t) - a)^2}, & G &= \frac{b^2\,(c\cosh(t) + a)}{c\cosh(t) - a}\\ L &= \frac{-ab^2c\cosh(t)}{\left(c^2\cosh^2(t) - a^2\right)(c\cosh(t) - a)}, & N &= \frac{-b^2}{c\cosh(t) - a}\\ k_1 &= \frac{-c\cosh(t)}{a(c\cosh(t) + a)}, & k_2 &= \frac{-1}{c\cosh(t) + a}\\ H &= \frac{-1}{2a}, & K &= \frac{c\cosh(t)}{a\,(c\cosh(t) + a)^2}.\end{aligned}$$

The geodesic curvature of a parallel is

$$k_g = \frac{-c\sinh(t)}{b\big(c\cosh(t) + a\big)}.$$

The total curvature is

$$\int_{\boldsymbol{z}_2} K \mathrm{d}\sigma = c(v_2 - v_1) \left. \frac{\sinh(t)}{\sqrt{c^2 \cosh^2(t) - a^2}} \right|_{t_1}^{t_2}.$$

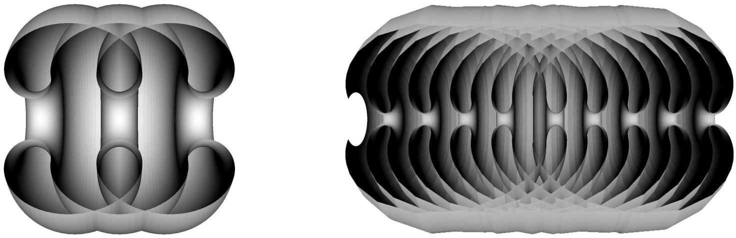

Figure 10. Left: Closed nodoid (compact without boundary), connected sum of four tori. Right: Connected compact nodoid with boundary.

Fig. 10 illustrates the versatility of the parameterization of nodoids adopted here. We avoid the periodic extension of nodoids with both positive and negative Gaussian curvature, maintain the orientability, preserve the C^∞ class and find new surfaces both closed and with boundary.

4. Applications

Comparison between theoretical/numerical predictions and experiments is of great interest. An experimental system has been developed [9] in which charge-stabilized emulsions are created in the form of capillary bridges, these are structures in which a drop of liquid A, immersed in liquid B, spans the gap between two parallel flat glass surfaces. The surface separating the two liquids has the topology of a cylinder and necessarily has a constant mean curvature determined by the Laplace pressure difference between the inside (A) and the outside (B) liquids.

In [1] we analyze and simulate numerically the structure of the crystalline ground state of particles strictly confined to a Delaunay surface and interacting with a pairwise-repulsive short-range power law potential. To determine candidate minimum energy configurations we use the Forces Method [2] in which we choose a certain number of particles and an initial configuration for them, then update the positions of the particles on the surfaces until a minimum energy configuration is reached. This occurs when the gradient of the potential energy created by the particles is orthogonal to the surface.

We are particularly interested in the defect structure of the ground state and how distinctive defect motifs emerge as the total curvature is varied within one class of Delaunay surfaces. We also aim to analyze the evolution of defects by tracking the ground state when the capillary bridge spans between two parallel flat surfaces. This incompressible movement plays with the most characteristic property of the Delaunay surfaces of having minimum lateral area.

The simplicity of the parameterization of the Delaunay surfaces presented here, has made possible to obtain the ground state on these surfaces for a large number of particles (never addressed before), and are also responsible of been able to analyze the case of nodoids in depth, never done before, due to the difficulty of other parametrizations used in their description, as well as obtaining families of Delaunay surfaces with a given volume.

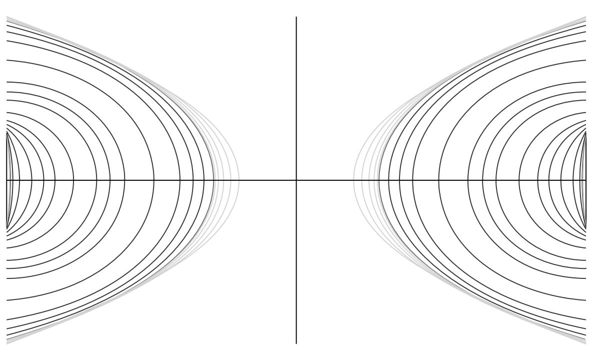

Figure 11. Planar sections containing the revolution axis of a family of Delaunay surfaces with constant volume. From the outside-in: cylinder, unduloids, catenoid, nodoids, catenoid and unduloids.

In Fig 11 we present planar sections that contain the common axis of revolution of several Delaunay surfaces with enclosed volume equal to 1 and radius 1 at the boundaries. Note that the solutions depend on t_0.

Here we illustrate the simplicity of our formulation by finding a surface which satisfies these conditions. Consider a plane curve $(f(t), g(t))$. The volume enclosed by its surface of revolution is given by $\pi \int_{t_0}^{t_1} f^2(t)g'(t)\mathrm{d}t$ and the end points by $(f(t_0), g(t_0)) = (f_0, g_0)$ and $(f(t_1), g(t_1)) = (f_1, g_1)$.

Consider for example the symmetric nodoid generated by a roulette C such that the enclosed volume is 1 and the radius is 1 at the end points $\pm t_0$. The equations to solve for a and b are then

$$\pi a b^4 \int_{-t_0}^{t_0} \frac{(c\cosh(t) - a)}{(c\cosh(t)+a)^2 \sqrt{c^2\cosh^2(t) - a^2}} \mathrm{d}t = 1$$

$$\frac{b\,(c\cosh(t_0) - a)}{\sqrt{c^2\cosh^2(t_0) - a^2}} = 1.$$

Once known the semiaxis of the underlying conic and the interval of parameterization of a meridian, we have all the ingredients to operate on the surface and understand its properties.

Acknowledgements

This work has been partly supported by the Spanish Research Council (Comisión Interministerial de Ciencia y Tecnología,) under project MTM2010-19660. The work of M.B. was also supported by the National Science Foundation through Grant # DMR-1004789 and by funds from the Soft Matter Program of Syracuse University.

References

[1] Bendito E., Bowick M., Medina A. and Yao Z., *Crystalline Particle Packings on Constant Mean Curvature* (*Delaunay*) *Surfaces*, Physical Review **88** (2013) 012405.

[2] Bendito E., Carmona A., Encinas A., Gesto J., Gómez A., Mouriño C. and Sánchez M., *Computational Cost of the Fekete Problem I*: *The Forces Method*, J. Comput. Phys. **228** (2009) 3288-3306.

[3] Besant W., *Notes on Roulettes and Glissettes*, Bell and Co., Deighton 1890.

[4] Delaunay C., *Sur la surface de revolution dont la courbure moyenne est constante*, J. Math. Pures et Appliquées **6** (1841) 309–320.

[5] do Carmo M., *Differential Geometry of Curves and Surfaces*, Prentice Hall, New Jersey 1976.

[6] Eells J., *The Surfaces of Delaunay*, Math. Intelligencer **9** (1987) 53–57.

[7] Hadzhilazova M., Mladenov I. and Oprea J., *Undoloids and their Geometry*, Archivum Matematicum (Brno) **43** (2007) 417–429.

[8] Hsiang W. and Yu W., *A Generalization of a Theorem of Delaunay*, J. Diff. Geom. **16** (1981) 161–177.

[9] Irvine W., Vitelli V. and Chaikin P., *Pleats in Crystals on Curved Surfaces*, Nature **468** (2010) 947-951.

[10] Kenmotsu K., *Surfaces of Revolution with Prescribed Mean Curvature*, Tôhoku Math. J. **32** (1980) 147–153.

[11] Koiso M. and Palmer B., *Rolling Construction for Anisotropic Delaunay Surfaces*, Pacific J. Math. **234** (2008) 345–378.

[12] Mladenov I., *Delaunay Surfaces Revisited*, C. R. Bulg. Acad. Sci. **55** (2002) 19–24.

[13] Rosseman W., *The First Bifurcation Point for Delaunay Nodoids*, Experimental Mathematics **14** (2005) 331–342.

Enrique Bendito and Agustín Medina
Departament de Matemàtica Aplicada III
Universitat Politècnica de Catalunya
Barcelona, SPAIN
E-mail address: `enrique.bendito@upc.edu`

Mark J. Bowick
Physics Department
Syracuse University
Syracuse, NY 13244-1130, USA
E-mail address: `bowick@phy.syr.edu`